

# Temperature Dependence of EFG Tensor in TCP Metals

B. C. Rai<sup>1</sup>, A. Kumar<sup>2</sup>

P.G. Centre, Department of Physics, College of Commerce, Arts and Science, Patna, India

Work completed in 2013 during Kumar's doctoral work.

<sup>1</sup>Corresponding author: Dr. B. C. Rai, Associate professor, College of Commerce, Arts and Science, Patna-20, India  
Email:bcraiphy@gmail.com

**Abstract:** Electric field gradient (EFG) tensor arises out of asymmetry in charge distribution around a nucleus in atoms, molecules and crystals. In case of metallic crystals, inhomogeneous electric field can result both due to ions and electrons. The conduction electrons and core orbital electrons in polarized probe produce an electronic EFG, while distant ions produce lattice EFG at probe's nucleus. The total EFG is the sum of these two terms, and is usually obtained by standard experimental methods. By performing lattice summations one gets lattice EFG. The electronic EFG is obtained by subtracting the lattice EFG from the total EFG. In this work, we obtain both the lattice and electronic contribution theoretically for tetragonal close packed (TCP) metals at several temperatures. Effect of core polarization has been accounted by using Sternheimer anti shielding factor, and that of temperature on EFG is obtained through temperature-variation in axial ratio ( $c/a$ ) of the metal concerned. Calculations for In and Sn indicate that EFG does not follow the usual  $T^{3/2}$ -law in TCP metals above 100 K. As the axial ratio tends towards unity, total EFG in these metals tends towards zero.

**Keywords:** Electric field gradient, tetragonal close packed metals, charge shift model, temperature dependence of EFG, Indium, Tin, three-half law

## 1. Introduction

The inhomogeneous electric field at probe nuclear site is described by electric field gradient which appears in interaction energy term in interaction of electric field with quadrupole moment of nucleus of probe for the cases of  $I > 1/2$ . This interaction splits nuclear energy levels of probe and leads to spectroscopic methods of measuring EFG, such as nuclear magnetic resonance, microwave spectroscopy, electron paramagnetic resonance, nuclear quadrupole resonance, Mössbauer spectroscopy or perturbed angular correlation. The splitting magnitude is sensitive to EFG values that mainly involve charges chiefly in the immediate vicinity of probe as EFG falls as inverse cube of distance. This fact is exploited in study of charge transfer in substitution, weak interaction and non-cubically symmetric charge distribution. In this work, we consider EFG at nuclear site in TCP metals which are non-cubic.

In non-cubic ionic lattice, asymmetric electronic and ionic environment produce EFG at a nuclear site. Several approaches appear in literature for calculating EFG using methods such as band structure, OPW, APW, tight binding, pseudo potential model, etc.[1-4] Though these provide elegant theoretical footing, surely these pose formidable problems in terms of actual calculation of exact wave functions. A phenomenological model known as *Charge shift model* for EFG was initiated by Bodenstedt and Persheid [5] for hcp (*sp*) metal that was a very

successful point charge model without using wave functions. Verma et al extended it to include transition metals with hcp lattices [6, 7] and its applicability regions were investigated by Gupta et al [8]. The method was recently used to calculate cohesive energy [9-12]. We developed similar model for the tetragonal close packed crystals for the first

time. Calculation for EFG in Indium competes well with experiments [13]. Recently one of us used it for EFG in Sn [14] using different lattice sum technique. Asymmetry in one of the electronic sub-lattices was also recently reported [15]. An important aspect of the model is that it takes into account the effect of temperature on lattice spacing as well as on conduction electron distribution around ions by using temperature dependent axial ratio. The efficacy of the model in EFG computation is thus tested; we have developed formulation for TCP metals and used in present work. The main focus is to bring out some essentials of temperature dependence of EFG rather than its exact values.

## 2. The Electric Field Gradient in TCP metals

TCP metals are three dimensional repetition of unit cells called tetragonal close packed (tcp or bct) unit cells which are characterized by interfacial right angles, and lattice parameters  $a=b \neq c$ . The axial ratio ( $c/a$ ) differs from the ideal value of  $\sqrt{2}$  from one metal to another and from one temperature to another for the same metal. The conduction electrons are contributed by ionizations at lattice sites, and probability of their being found at a position smears according to amplitude square of their wave functions. However exact wave functions of such a large number of electrons in infinite lattice are rare. We may mark small pockets where they are more likely to be found by energy minimization. In charge shift model, conduction electrons are assumed as tiny spheres located midway between the ions forming the first co-ordination cell of an ion. The electronic planes act as glue and metallic bonding results.

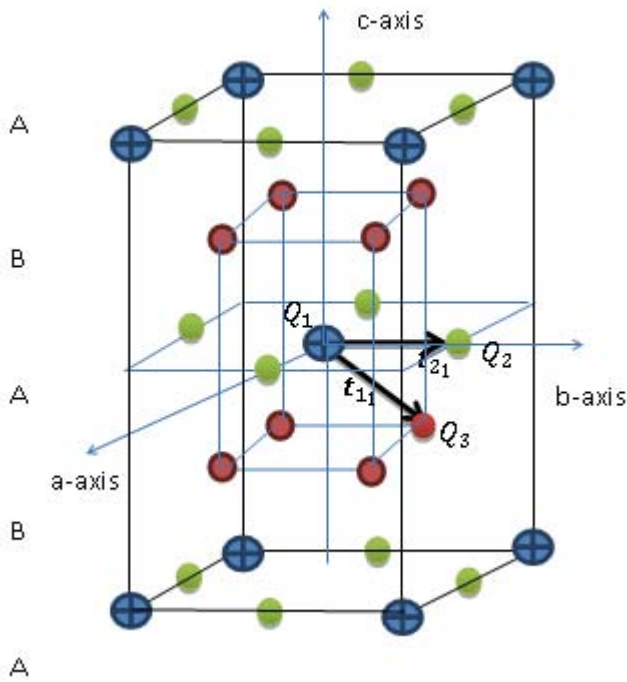


**Figure 1:** Non-equivalent sites (3) and planes (2) in tcp metals

The crystal symmetry gives two non-equivalent electronic sites (2 and 3) forming two non-equivalent planes perpendicular to the c-axis: *mixed plane*(A) that is composed of ions and one type of conduction electron spheres (2), while *pure plane*(B) that consists purely of the remaining type of conduction electron spheres(3). The ionic charge is denoted by  $Q_1 = Z_{eff}e$ , where  $e$  is modulus of electronic charge, and  $Z_{eff}$  is consistent with extra-ionic electronic wave functions (ionization).

The total conduction electronic charge donated per ion ( $-Z_{eff}e$ ) is equally distributed among the twelve electronic sites in the *first co-ordination cell*, to start with, forming half of the total charge at a site. The other half comes from the other partner ion. Thus, the charge at one electronic site in this way is ( $-\frac{Z_{eff}e}{6}$ ). The interaction energy calculation using this distribution gives a minimum at ideal value of axial ratio for tcp. A *shift* of charge is performed for restoring *actual axial ratio* by means of an extra stress of electrostatic origin. A fraction  $\delta$  of charge is *shifted* so as to make the charge at one site in *pure plane* equal to ( $-\frac{Z_{eff}e}{6})(1 - \delta)$ . The charge resulting from this activity on electronic site in *mixed plane* is obtained by electrical neutrality of unit cell. The charge on a conduction electron sphere in mixed planes(A) is denoted by  $Q_2$ , and in pure plane (B) by  $Q_3$ . Using the site contribution counting, the electrical neutrality for the unit cell is embodied in the following equation

$$\frac{1}{4}[8Q_2] + \frac{1}{2}[4Q_3] + 8Q_3 + 2Z_{eff}e = 0 \quad (2)$$

The charge transfer quantified by the factor  $\delta$  yields the charges as follows:

$$Q_2 = -\frac{1}{6}Z_{eff}e(1+2\delta) \quad (3-i)$$

$$Q_3 = -\frac{1}{6}Z_{eff}e(1-\delta) \quad (3-ii)$$

The numerical evaluation of factor  $\delta$  is done by considering the elasticity and the electrostatics of the unit cell as follows. The charges resulting due to the *shift* produce an *electrostatic stress* that brings the ideal unit cell to the actual shape and size. The same can be affected by *mechanical stress* also. The two approaches are made consistent and  $\delta$  is expressed in terms of compliance co-efficient  $S_{ij}$  for the element under study. The derivation and work concerned is the same as we reported earlier [13]. We get for TCP systems,

$$\delta = \frac{(\frac{\epsilon}{a} - \sqrt{2})}{\sqrt{2}} \cdot \frac{54 \epsilon_0 a^4}{(Z_{eff}e)^2 (2S_{33} - S_{12} - S_{11})} \dots (4)$$

Thus, using equations (3) and (4), the charge distribution in the whole crystal is obtained. Using these charges, one can obtain electric field gradient.

The **electric field gradient tensor** is a nine component entity  $V_{ij}$  given as

$$V_{ij} = \frac{\partial^2 \phi}{\partial x_i \partial x_j}$$

Here  $\phi$  is the potential due to charge distribution. For principal axes as X-, Y- and Z-axes, the cross terms in the EFG matrix vanish, and diagonal elements sum to zero (tracelessness). Only two elements are thus independent and asymmetry parameter is given by

$$\eta = \frac{V_{xx} - V_{yy}}{V_{zz}}$$

In this expression  $|V_{zz}| > |V_{yy}| > |V_{xx}|$ , which means asymmetry parameter is between zero and one. For TCP lattice, we take c-axis as Z-axis, a- and b-axes as X- and Y-axes, which are identical and asymmetry parameter is zero. We are thus for  $V_{zz}$  only.

The electric field gradient at vacant nuclear site of probe is first evaluated, and then the effect of probe core polarization is taken into account.

Let us take a charge  $q$  at position  $\vec{r}$  relative to an ionic site as origin of co-ordinates in the crystal. It produces electric field intensity at the origin whose space rate of variation along c-axis which is our Z-axis, is the electric field gradient along c-axis, which is given by

$$V_{zz} = \frac{q}{4\pi \epsilon_0} \frac{3z^2 - r^2}{r^5} \dots (5)$$

In the tcp lattice, crystallo-physical co-ordinates of sites in the ion's lattice are denoted by real number triplets  $(n_1, n_2, n_3)$  in units of lattice parameters  $a, a,$  and  $c$ . Taking (000) at the interstitial ion in the unit cell, co-ordinates for the nonequivalent sites are obtained. Using these co-ordinates, the position of a site in any other unit cell may be written.

*Notations:*

$N_i = n_i + t_{ijk}$  denotes i-th component of position vector of nonequivalent charge located at k-th position of j-th nonequivalent type site in n-th unit cell ( $i = 1$  for x-component, 2 for y-component and 3 for z-component). The multiplicity per unit cell for j-th non-equivalent site is denoted by  $M_j$ .

In this notation system, the position vectors may be written as

$$\mathbf{r} = \sum N_i \mathbf{u}_i$$

The vectors  $\mathbf{u}_i$  are the unit vectors along co-ordinate axes. The position vector of a site in TCP system is, thus, given by

$$\mathbf{r} = (n_1 + t_{1jk}) \mathbf{u}_1 + (n_2 + t_{2jk}) \mathbf{u}_2 + \left(\frac{c}{a}\right) (n_3 + t_{3jk}) \mathbf{u}_3.$$

The charges given in equations (2) and (3) and positions given here are fed for EFG in equation (5) and lattice sum is performed. Accordingly, with these notations, the EFG may be written as

$$V_{zz} = \sum_{j=1}^3 Q_j b_j$$

The lattice sum is contained in  $b_j$ , where

$$b_j = \frac{e}{4\pi\epsilon_0 a^3} B_j$$

$$B_j = \sum_{n_3} \sum_{n_2} \sum_{n_1} \sum_{j_k=1}^{M_j} \frac{3N_j^2 - (N_1^2 + N_2^2 + N_3^2)}{(N_1^2 + N_2^2 + N_3^2)^{2.5}} \dots \quad (6)$$

It may be observed that the lattice sums given by equation (6) depend only upon axial ratio ( $c/a$ ) contained in writing  $N_3$ .

The coefficients  $B_j$  are obtained by the lattice summations methods. The conditional convergence of lattice sums for evaluation of EFG pose problems, and hence much care has been taken in this direction by using various lattice sum methods [16-18]. We have used here a plane wise summation procedure; we consider a particular plane normal to  $c$ -axis, that bears the fourfold symmetry here, sum over all the sites and then do the same for the next plane, and so on. All these sums are added together to give the lattice sum.

The net EFG at nuclear site due to ionic and electronic sites can, thus, be calculated.

The atomic core of probe nucleus that is put now in the crystal field at the origin interacts with the field gradient and gets polarized (core polarization). The splitting its energy levels is strongly dependent on the degree of deviation of wave functions from free state. To account for this, one uses Sternheimer's factor ( $1 - \gamma_\infty$ ) for ions and conduction electrons [19 and 20]. Thus we use

$$eq = \left(\sum_{j=1}^3 Q_j B_j\right) (1 - \gamma_\infty) \frac{e}{4\pi\epsilon_0 a^3} \dots \quad (7)$$

The three dimensionless lattice sums  $B_j$  in the above equation are independent of the lattice parameter  $a$ , and depend only on the axial ratio  $c/a$  of the crystals with interfacial angles  $90^\circ$ . The charges  $Q_j$  and anti-shielding factor [20] are dependent on the element concerned.

The experimental value of EFG is extracted from the measurement of the frequency and the quadrupole moment. It is known that the experimental techniques are not free of error bars. Hence electronic contribution to EFG has always been open to question as ionic contribution comes from lattice summation and electronic one is obtained by a subtraction. In the model at hand, both the ionic and the electronic EFG are calculable using lattice summations.

### 3. Temperature Effect

The theoretical approaches to thermal effects in condensed state are almost phenomenological. Although a multitude of microscopic motion are temperature linked, such as conduction electronic translation, lattice vibration, partial molecular rotation, upper energy-state excitation, and anomalous effects, several of these are *frozen* case wise in metals. The electron with high frequency (of the  $10^{15}$  Hz order) is approximated to remain almost un-followed by slow ions (of frequency order  $10^{13}$  Hz) in the Born-Oppenheimer (adiabatic) approximation, allowing a *non-phonon* treatment. For the case, ionic part of EFG originates from temperature-expansion of crystals. The temperature effect on EFG is believed to originate from change in lattice spacing, nature of lattice vibration, probe core polarization and conduction electrons.

In equation (7), the lattice sums are functions of  $c/a$ , which in turn are temperature dependent. This takes care of temperature-expansion of crystal. As conduction electron tiny spheres lie midway between ions in the first co-ordination cell, their lattice is also temperature expanded. This forms one part for electronic EFG; the other part comes through changes in charges in equations (3) due to temperature dependent  $\delta$  in equation (4). Thus, equation (7) may be separated into electronic and lattice parts of EFG as

$$eq_{lat}(T) = [Z_{eff} B_1(T)] (1 - \gamma_\infty) \frac{e}{4\pi\epsilon_0 a^3} \dots \quad (8)$$

$$eq_{el}(T) = [Q_2(T) B_2(T) + Q_3(T) B_3(T)] (1 - \gamma_\infty) \frac{e}{4\pi\epsilon_0 a^3} \dots \quad (9)$$

One must note that equations (8) and (9) give us EFG along  $c$ -axis that we have taken as  $Z$ -axis, and hence may be positive or negative. These may be used to relate signs and magnitudes and study EFG systematics as temperature is changed.

### 4. Numerical Computation

For numerical computations, co-ordinates of TCP lattice points and electronic sites within unit cell are obtained [14, 15]. The lattice sums  $B_j(T)$  of equation (6) are evaluated for  $c/a$ -values available in literature at several temperatures ( $T$ ) and are used to get EFG at various temperatures (Tables 1 and 2).

**Indium:** The result in the Table 1 is based on lattice parameters for Indium at given temperatures [21]. It is found in this reference that the value of lattice spacing  $a$  goes on increasing monotonically but  $c$  first increases (4.2 K to 250K) and then decreases, though  $c/a$  continues to show decrement throughout the range (only  $c/a$  values are displayed in the table).

The sign of electronic EFG is positive and that of lattice EFG is negative, and total EFG is negative throughout the temperature range.

**Table 1:** Temperature effect on EFG in InIn

Temperature T(K)	Axial ratio	Lattice sums			Electronic EFG $eq_{el}(T)$ ( $\times 10^{21} \text{Vm}^{-2}$ )	Ionic EFG $eq_{lar}(T)$ ( $\times 10^{21} \text{Vm}^{-2}$ )	EFG ( $\times 10^{21} \text{Vm}^{-2}$ )
		B <sub>1</sub> (T)	B <sub>2</sub> (T)	B <sub>3</sub> (T)			
4.2	1.5315	-1.823	-6.829	4.558	1.1751	-5.5667	-4.3916
100	1.5296	-1.818	-6.825	4.552	1.1696	-5.5204	-4.3508
150	1.5288	-1.816	-6.824	4.550	1.1647	-5.4882	-4.3236
200	1.5272	-1.812	-6.821	4.545	1.1590	-5.4449	-4.2858
250	1.5245	-1.805	-6.816	4.537	1.1529	-5.3891	-4.2361
300	1.5207	-1.795	-6.810	4.525	1.1469	-5.3199	-4.1730
350	1.5152	-1.780	-6.801	4.507	1.1396	-5.2281	-4.0886
400	1.5081	-1.762	-6.789	4.484	1.1316	-5.1185	-3.9870

The plots of electronic EFG, lattice EFG and total EFG in Indium against temperature reveal more temperature dependent features (figures 2 and 3).

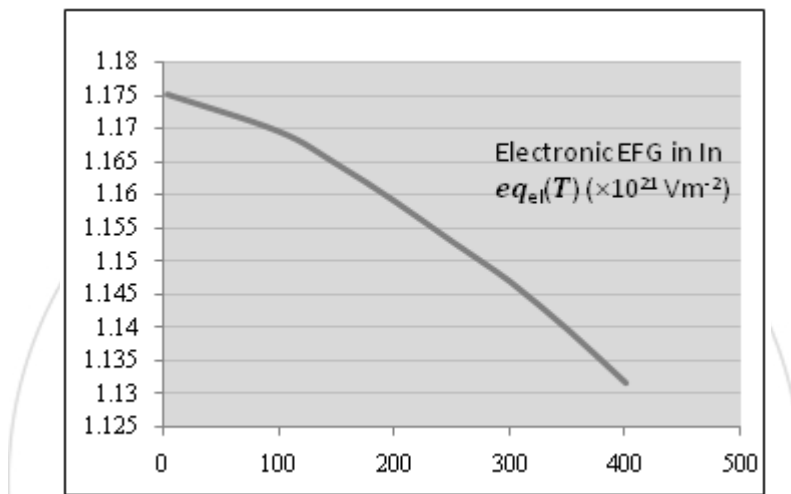


**Figure 2:** Electronic EFG in Indium as a function of temperature in Kelvin

We see that the electronic EFG decreases non-linearly while the lattice and total EFGs increase non-linearly, as the temperature is increased. At temperatures above 120 K, the deviation in the magnitude is more pronounced.

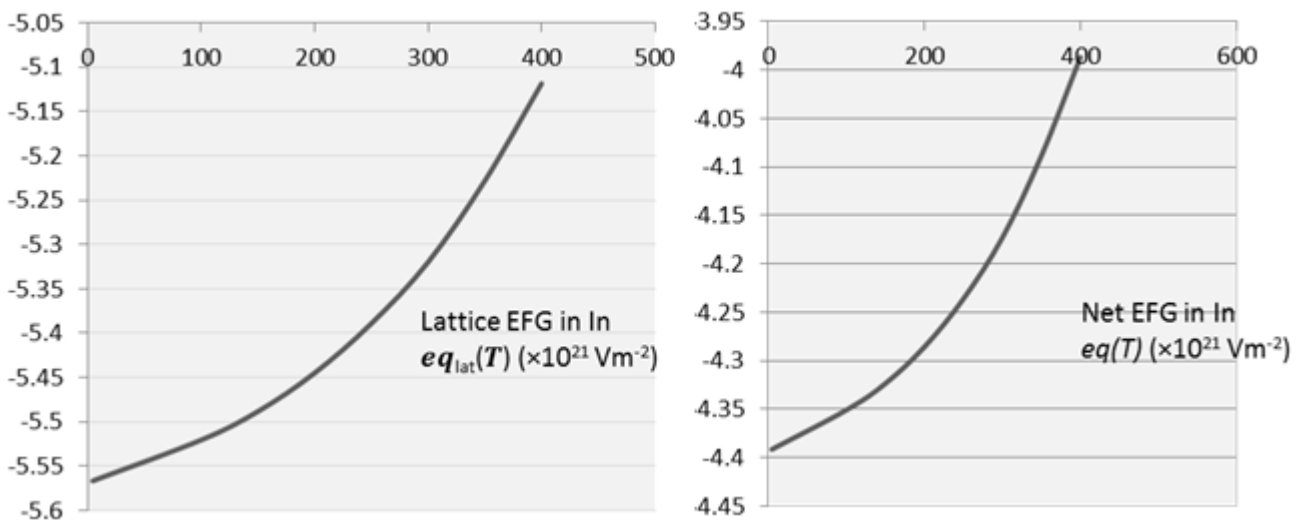


**Figure 3:** Lattice and net EFG in Indium as a function of temperature in kelvin

**Stannum :** Using the same algorithm as for Indium, we tabulate the electronic, lattice and total EFG in SnSnas function of temperature [Table 2] using data in ref [21,22]. The signs of electronic EFG, lattice EFG and total EFG are opposite to those in Indium. This may be attributed to the different values of axial ratios. In stannum, the electronic EFG changes sign in between the temperatures of 212 K and 300 K but lattice EFG and net EFG remain positive.

**Table 2:** Temperature effect on EFG in SnSn

Temperature T(K)	Axial ratio	Lattice sums			Electronic EFG $eq_{el}(T)$ ( $\times 10^{21} \text{ Vm}^{-2}$ )	Ionic EFG $eq_{lat}(T)$ ( $\times 10^{21} \text{ Vm}^{-2}$ )	EFG ( $\times 10^{21} \text{ Vm}^{-2}$ )
		$B_1(T)$	$B_2(T)$	$B_3(T)$			
33	0.54557	15.1412	-10.4836	-12.4122	-0.4795	5.1270	4.6475
106	0.54634	15.0504	-10.4651	-12.3794	-0.4848	5.0750	4.5902
148	0.54675	15.0019	-10.4553	-12.3611	-0.4883	5.0464	4.5581
166	0.54706	14.9653	-10.4478	-12.3477	-0.4904	5.0271	4.5368
178	0.54715	14.9558	-10.4459	-12.3441	-0.4914	5.0201	4.5287
180	0.54721	14.9479	-10.4440	-12.3411	-0.4916	5.0169	4.5254
186	0.54733	14.9347	-10.4410	-12.3360	-0.4924	5.0099	4.5175
194	0.54746	14.9185	-10.4380	-12.3300	-0.4932	5.0017	4.5085
200	0.54745	14.9202	-10.4388	-12.3309	-0.4937	5.0005	4.5068
212	0.54768	14.8920	-10.4331	-12.3208	-0.4949	4.9869	4.4920
300	0.913	0.64218	-0.62183	-1.56437	+0.2633	0.7799	1.0432

For temperature from 33 K to 212 K, we show the graphs of electronic, lattice and net EFGs (figures 4 and 5).

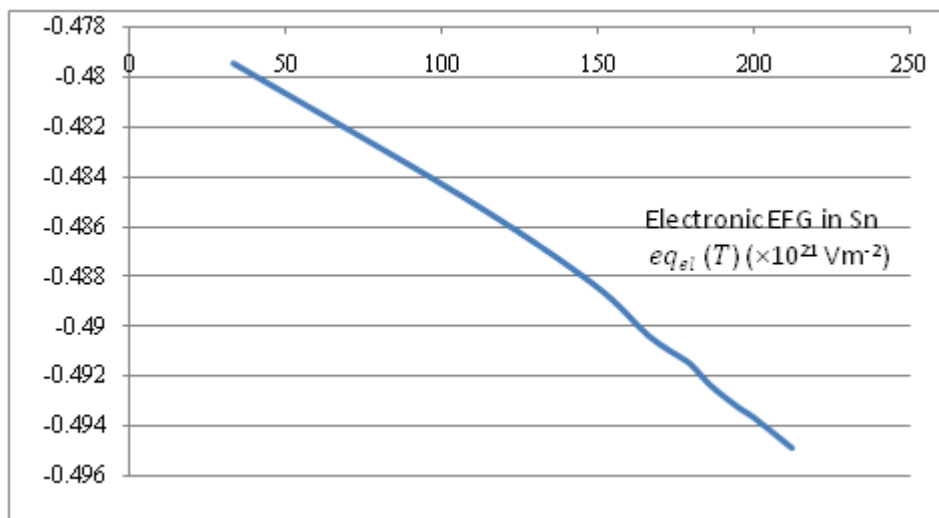


**Figure 4:** Electronic EFG in Stannum as a function of temperature in kelvin

The electronic EFG, negative in sign, goes on decreasing with temperature. The graph shows initial non-linearity and greater deviations at larger temperatures. The lattice EFG and total EFG have positive signs and show decrement as temperature increases. At temperatures above 120 K, deviations are more pronounced.

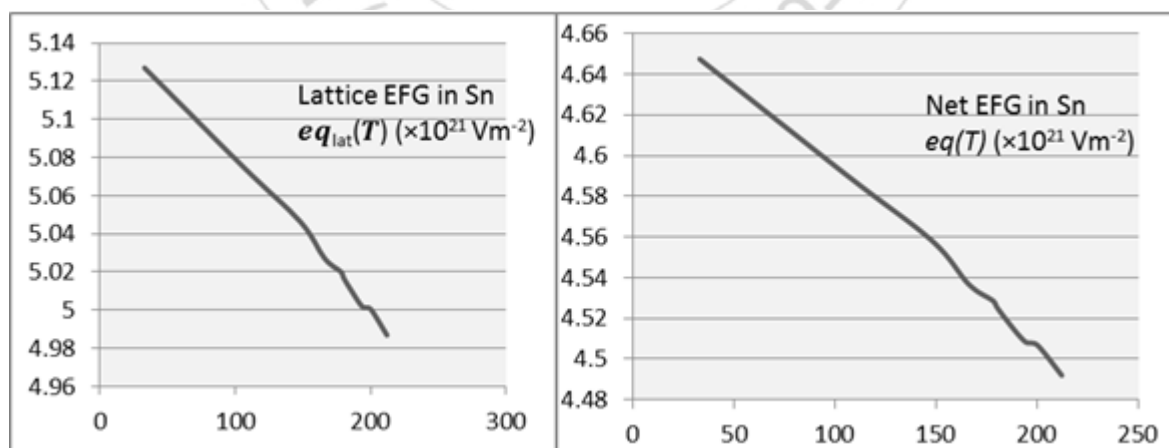


**Figure 5:** Lattice and net EFG in Stannum as a function of temperature in kelvin

## 5. Result and Discussion

Computations bring out essential features of temperature effect on EFG in TCP metals that compete with observations. Graphs of *electronic* EFG indicate its non-linear decrement as the temperature increases. Lattice EFG,

however, decreases in SnSn, but increases in InIn. This can be linked to opposite behavior of axial ratio in the two hosts as temperature increases. Anisotropy observed in thermal expansion is linked to the dominance of longitudinal mode over shear mode of lattice vibration as vibrational energy is increased by increasing temperature.

The temperature dependence is nearly linear below 120 K, and thereafter it is non-linear.

As temperature is increased, axial ratio change. The total EFG changes with axial ratio, and proceeds towards zero when axial ratio is extrapolated to unity. This is natural as body centered cubic lattice has vanishing EFG.

In light of the fact that temperature dependence of EFG is an informer of its origin, the results are interesting. In non-cubic non-transition metals EFG is believed to follow an empirical relation known in literature as  $T^{3/2}$ -law, given, in usual notations, by

$$e_q(T) = e_q(0) [1 - B T^{\frac{3}{2}}]$$

The behavior was observed by Christiansen and co-workers in 1976 in a number of available NQR data [23]. It was assumed to apply to several systems and universalized. To test if a tcp element obeys the  $T^{3/2}$ -law in a temperature variation from  $T_1$  K to next close temperature  $T_2$  K, we used the EFG change from  $e_q(T_1)$  to  $e_q(T_2)$ . Using the  $T^{3/2}$ -law,

$$\frac{e_q(T_2) - e_q(T_1)}{T_2^{3/2} - T_1^{3/2}} = -e_q(0)B$$

If the ratio on LHS of equation be found temperature independent for all available temperature data, the law is certainly obeyed.

Jena has attempted to relate electronic contribution using lattice vibrations, while Nishiyama *et al* consider mean square of displacements of ions in harmonic vibration; these explain the  $T^{3/2}$ -law [24 and 25]. However, the simplicity of the relation on one hand, and the strength of observed variation on the other, is a bit puzzling. The story of temperature dependence is not only that of mean square displacements of ions, as main contributor appear as distribution of charges in neighborhood of probe and conduction electrons [26].

Calculation in InIn and SnSn using obtained EFG shows that at temperature above 100 K, the above law is not satisfied. Our study on available data on fairly large number of other cases also suggests a departure from the  $3/2$ -law, especially in sp-band metals and probe-host sets, such as CdZn, ZnZn, CdIn, CdBi, CdCd, and on transition metallic systems, such as FeBe, CdRe, FeZr, CdZr, etc. [27]. Even in SnSn at high temperature, disagreement is observed. Thus, a single value of the exponent of T that fits the entire data seems under question mark. Some data may be analyzed by a quadratic rule or linear fit, while others seek an exponent of T different from 1.5, and are case dependent. A universal law is still missing.

## 6. Conclusion

Charge distribution in TCP metals given by charge shift model is used to calculate temperature dependent electronic, lattice and total EFG along c-axis. The total EFG changes with axial ratio, and proceeds towards zero when axial ratio is extrapolated to unity. This is natural as body centered cubic lattice has vanishing EFG. Results indicate that EFG depends non-linearly on temperature in several cases. Departure from  $T^{3/2}$ -law is indicated by calculations and curve fitting on different probe host sets.

## 7. Acknowledgement

Authors are thankful to Professor H C Verma, Department of Physics, I I T, Kanpur for fruitful discussions on temperature effects on EFG of several systems cited in the work.

## References

- [1] Das T.P., *Physica Scripta* 11, 121 (1975)
- [2] Mahapatra N.C, Patnaik P.C., Thomson M.D, Das T.P. *Phys. Rev. B* 16 30001(1977)
- [3] Coker A, Lee T and Das T P, *Phys. Rev B* 13, 55(1976)
- [4] Hygh E. H. and Das T. P., *Phys. Rev.* 143, 452(1962)
- [5] E. Bodenstedt and B Parscheid, *Hyp. Int.* 5, 291 (1978)
- [6] H.C. Verma and G.N. Rao, *Phys. Lett.* A82, 303(1981)
- [7] S. Chandra and H.C. Verma, *Phys. St. Sol. B* K73, 131 (1985)
- [8] S.N.Gupta, G.Verma and H.C Verma, *Pramana* 23, 39 (1984)
- [9] S.Chandra and H.C.Verma, *Phys. Rev.* B34, 9(1986)
- [10] S.Chandra and H.C.Verma, *Phys. St. Sol.*(b), 145(1988)K1
- [11] S.N. Gupta, A. Anand, S. Chandra and B. C. Rai, *Sanjivni Journals(JPS)* vol 1 no. 1,159-162 (2010)
- [12] S.N.Gupta, A. Anand, S. Chandra and B. C. Rai, *Sanjivni Journals(JPS)* vol 2, no. 2, 35-38 (2010).
- [13] H.C. Verma, B. Kumar, B. C. Rai and S. Chandra, *Hyp. Int.* 52, 97 (1989)
- [14] B C Rai, *I J P A*, ISSN 0974-3103 VOL 5 NO. 1, 33-39(2013)
- [15] B C Rai and A Kumar, *I J P A*, ISSN 0974-3103 vol 5 no 1, 25-32( 2013)
- [16] F. W. de Wette, *Phys. Rev.* 123, 1(1961)
- [17] D. P. Verma, A. Yadav and H. C. Verma, *Pramana* 21, 357(1983)
- [18] D. P. Verma, B. Kumar and H. C. Verma, *Pramana* 25, 211(1985)
- [19] T. P. Das and R. Bersohn, *Phys. Rev.* 102, 733 (1965)
- [20] R. M. Sternheimer, *Phys. Rev.*, 130, 1423(1963)
- [21] W B Pearson, *A Hand book of Lattice Spacing and Structures of Metals and Alloys*, vol 2, Pergamon Press.
- [22] G. S. Collins and N. Benczer-Koller, *Phys. Rev.* B17, 5(1978) 2085-97
- [23] J. Christiansen, P. Heubes, R. Keitel, W. Loeffler, W. Sandner and W. Wittihun, *Z.Phys.* B24 177 (1976)
- [24] P Jena, *Phy. Rev. Lett.*, 36,418(1976)
- [25] K Nishiyama and D Riegel, *Hyp. Int., Volume 4, Issue 1-2, pp490-508(1978)*
- [26] W. Semmler, P. Raghvan, M Senba and R.S. Raghvan, *Hyp. Int.* 9 323-328 (1981)
- [27] R Vianden, *Hyp. Int.* 10,1243(1981)